ANL-80-34

ANL-80-34

BIAXIAL CREEP-FATIGUE BEHAVIOR OF MATERIALS FOR SOLAR THERMAL SYSTEMS

by

S. Majumdar

ARGONNE NATIONAL LABORATORY

ARGONNE NATIONAL LABORATORY, ARGONNE, ILLINOIS

Prepared for the U. S. DEPARTMENT OF ENERGY
under Contract W-31-109-Eng-38

DISCLAIMER

Printed in the United States of America
Available from
National Technical Information Service
U. S. Department of Commerce
5285 Port Royal Road
Springfield, VA 22161

NTIS price codes
Printed copy: A03
Microfiche copy: A01

Distribution Category:
Solar Thermal--Large Scale Systems
(UC-62c)

ANL-80-34

ARGONNE NATIONAL LABORATORY
9700 South Cass Avenue
Argonne, Illinois 60439

BIAXIAL CREEP-FATIGUE BEHAVIOR OF MATERIALS FOR SOLAR THERMAL SYSTEMS*

by

S. Majumdar

Materials Science Division

May 1980

*Work supported by the U. S. Department of Energy under Sandia Contract No. 85339 for the Solar Thermal Program.

THIS PAGE

WAS INTENTIONALLY

LEFT BLANK

TABLE OF CONTENTS

LIST OF FIGURES

LIST OF FIGURES (CONTD.)

LIST OF TABLES

BIAXIAL CREEP-FATIGUE BEHAVIOR OF MATERIALS FOR SOLAR THERMAL SYSTEMS

by

S. Majumdar

ABSTRACT

Biaxial creep-fatigue data for Incoloy 800 and Type 316H stainless steel at elevated temperature are presented. Tubular specimens were subjected to constant internal pressure and strain-controlled axial cycling with and without hold times in tension as well as in compression. The results show that the internal pressure affects diametral ratchetting and axial stress range significantly. However, the effect of a relatively small and steady hoop stress on the cyclic life of the materials is minimal. A 1-min compressive hold per cycle does not seriously reduce the fatigue life of either material; a tensile hold of equal duration causes a significant reduction in life for Type 316H stainless steel, but none for Incoloy 800. Fracture surfaces of specimens made of both materials were studied by scanning electron microscopy to determine the reason for the difference in behavior.

I. INTRODUCTION

A general feature of solar thermal systems that is distinctly different from the operating conditions associated with fossil and nuclear power plants is the highly cyclic nature of the thermal loading experienced by critical components. Solar thermal systems will undergo at least one major start-up and shutdown cycle per day, with additional cycles likely to be imposed by intermittent cloud cover and unscheduled maintenance and repair. Thus, critical components may be expected to accumulate of the order of tens of thousands of cycles over their design lifetime. In many cases, such as the solar central receiver, the temperatures and stresses will be sufficiently high to introduce creep-fatigue-environment interaction as a major life-limiting factor. A further complicating factor in many solar thermal systems is the highly asymmetric nature of the thermal load, which together with the pressure load often results in the creation of a multiaxial state of stress in critical components of a solar system. Unfortunately, virtually no multiaxial creep-fatigue data are currently available for any material.

The present program was initiated in order to address the problem of creep-fatigue under a biaxial state of stress. The materials chosen were Type 316H stainless steel and Incoloy 800, both of which are candidate materials for use in solar thermal systems. Tubular specimens were subjected to a constant internal pressure and strain-controlled axial cycling with and without hold time at elevated temperature. The data generated for Type 316H stainless steel have been published in detail in a previous report.[1] The present report summarizes the results obtained for Incoloy 800 and compares the observed behavior with that of Type 316H stainless steel.

II. EXPERIMENTAL DETAILS

Details of the specimen design and test equipment were described in Ref. 1. Specimens were fabricated from 1-in.-diameter seamless tubing supplied by Pacific Tube Company of Los Angeles, California; tube dimensions were 1-in. OD x 0.109-in. (min) wall for Type 316H stainless steel and 1-in. OD x 0.125-in. wall for Incoloy 800. Chemical analysis of the Type 316H stainless steel was described in Ref. 1; similar data for Incoloy 800 are given in Table I. The Incoloy 800 tubing was given an annealed and pickled finish by the vendor and satisfied ASME specification SB-163. All the specimens were tested in the as-received condition. Nominal room-temperature mechanical properties of both the materials, as supplied by the vendor, are given in Table II. Micrographs of the as-received materials, shown in Fig. 1, indicate that the grain structures are generally equiaxed with average ASTM grain sizes of 6.5 and 6.3 in transverse section and 6.4 and 5.9 in longitudinal section for Type 316H stainless steel and Incoloy 800, respectively. Note that the grain size for the Incoloy 800 material is rather large and consequently the present heat may not be representative of an average heat of Incoloy 800.

The biaxial fatigue testing was carried out in a closed-loop servo-controlled MTS testing machine using constant internal pressure and axial strain control. The internal pressure was provided by commercially available pressurized air bottles. Axial and diametral strains were measured by means of high-temperature extensometers and the axial load was measured by a 40-kips load cell. The specimen was heated by a Lepel induction heater operating at a frequency of 455 kHz. The maximum temperature variation in the central 0.5-in. gauge length of the specimen was $\pm$10°F.

The test procedure consisted of first heating the specimen to the desired temperature with zero axial load, and holding the temperature steady until the whole system came to thermal equilibrium. The internal pressure, if any, was then applied and the specimen kept at the temperature for sufficient time to allow the new temperature distribution to reach equilibrium. The specimen was then cycled axially under axial strain control. Hysteresis loops of axial stress versus axial strain and axial strain versus diametral strain were recorded on x-y plotters at regular intervals. Each individual signal was also plotted on a strip-chart recorder. For the internally pressurized specimens, the test was shut down automatically when a crack penetrated through the wall. For the unpressurized specimens, the test was shut

Table I. Composition of Incoloy 800 Seamless Tubing (Heat HH 7326A)

Element	Content, wt %		
	Ladle Analysis	Check Analysis Specimen From	
		Test 1053	Test 1064
C	0.02	0.023	0.020
Mn	0.76	0.64	0.65
S	0.002	-	-
Si	0.44	0.40	0.49
Ni	34.34	34.26	34.10
Cr	31.28	21.25	21.25
Ti	0.44	0.37	0.38
Cu	0.06	0.03	0.03
Al	0.29	0.20	0.21
Fe	42.37	42.77	42.82

Table II. Nominal Room-temperature Mechanical Properties of Type 316H Stainless Steel and Incoloy 800 Tubing

Material	Ultimate Strength, ksi	Yield Strength, ksi	% Elongation	Rockwell Hardness	Grain Size, ASTM No.
Type 316H Stainless Steel Heat 180124	85.25	46.33	65	76-80	6
Incoloy 800 Heat HH7326A	80.46	41.97	54	77	6

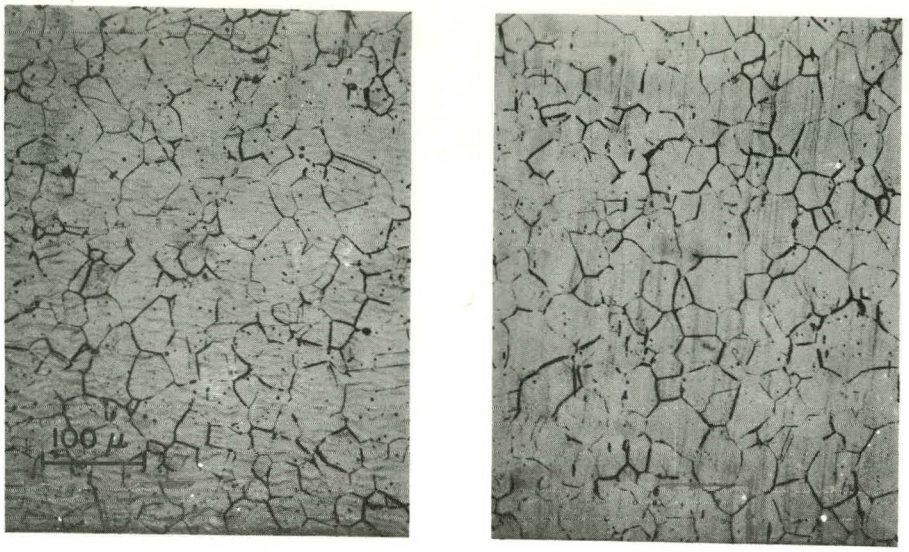

(a)

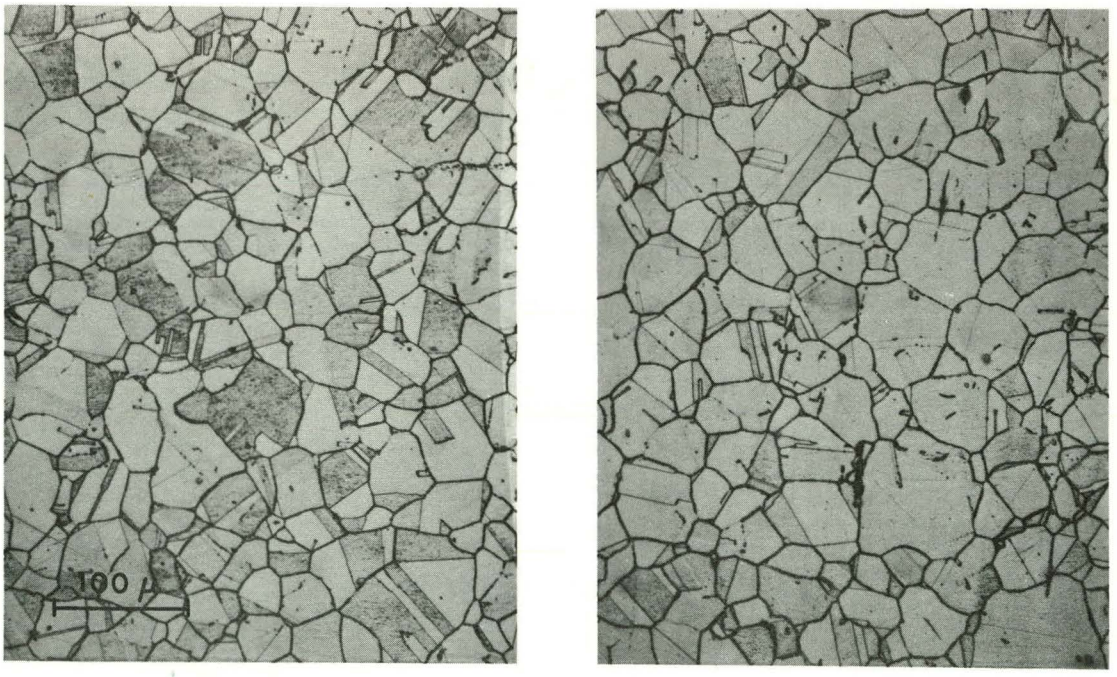

(b)

Fig. 1. Typical Microstructure of (a) Type 316H Stainless Steel and (b) Incoloy 800 in the As-received Condition. Transverse sections on left, longitudinal sections on right.

down automatically when a crack penetrated through the wall. For the unpressurized specimens, the test was shut down automatically when the specimen fractured. The number of cycles to failure was determined from the diametral-strain strip-chart recording at the onset of rapid change in the diametral strain. No attempt was made to measure crack lengths in the specimens. Some of the fractured specimens were studied using scanning electron microscopy.

III. TEST RESULTS

All testing was carried out at a total axial strain range of 0.5% and at a temperature of 1100°F. Internal pressures of 0, 1100, and 2000 psi were used together with 0, 1-min tensile and 1-min compressive hold times (at the maximum axial strain limit).

A summary of all the biaxial tests conducted on Type 316H stainless steel and Incoloy 800 are shown in Tables III and IV, respectively. The plastic strain range, diametral strain range, and axial stress range reported in the tables are those that were measured at approximately half life for each test. The axial plastic strain range was calculated from the total axial strain range and stress range by the following relation:

$$\Delta\varepsilon_p = \Delta\varepsilon_t - \frac{\Delta\sigma}{E} ,$$

where

$$E = \begin{cases} 22.2 \times 10^6 \text{* psi for Type 316H stainless steel;} \\ 22 \times 10^6 \text{ psi for Incoloy 800.} \end{cases}$$

The hoop-stress values reported in the tables were computed by the thin-wall tube approximation formula using the average radius of the tube. The diametral strains reported are the calculated hoop strains at the outer surface, obtained by dividing the measured diametral displacements by the outside diameter of the specimen at the gauge section.

At a test temperature of 1100°F and axial strain rates of 1×10^{-3} - 4×10^{-3}/s, Incoloy 800 exhibits unstable jerky flow for the first few cycles, as shown in Figs. 2 and 3. This is associated with dynamic strain aging in the material. However, after a few cycles ($\sim$ 10) the material hardens and the unstable behavior disappears. Tests conducted on Type 316H stainless steel under identical conditions do not exhibit such unstable behavior, as shown in Fig. 4.

Hysteresis loops at the tenth cycle and at approximately half-life for unpressurized specimens of Incoloy 800 with 1-min compressive and tensile hold are shown in Figs. 5 and 6, respectively. Similar plots for pressurized specimens are shown in Figs. 7-9 (1100 psi) and Figs. 10-11 (2000 psi).

---

*In test 1098, which was carried out at room temperature, $E = 27 \times 10^6$ psi.

Table III. Summary of Biaxial Creep-fatigue Tests of Type 316H Stainless Steel (Axial Strain Rate = 4×10^{-3}/s)

Test No.	Internal Pressure, ksi (MPa)	Hold[a] Time, min	Axial Strain Range, %		Diam Strain Range, %	Axial Stress, ksi (MPa)		Hoop Stress, ksi (MPa)	Cycles to Failure	Mean Diam Strain at Failure, %	No. of Initiation Sites
			Total	Plastic		Range	Mean				
997	0	0	0.51	0.19	0.20	71.5 (493)	0.1 (1)	0	14156	-0.02	1
999	0	0	0.50	0.19	0.19	70.1 (483)	0	0	8110	-0.02	2-3
1035	0	1C	0.49	0.16	0.21	75.1 (518)	1.1 (7)	0	9750[b]	-0.06	-
1052	0	1C	0.50	0.18	0.19	74.0 (510)	1.7 (12)	0	13518	-0.10	5
1001	1.1 (7.6)	0	0.50	0.17	0.19	74.3 (512)	0.7 (5)	6 (41)	15566	+1.05	1
1012	1.1 (7.6)	0	0.50	0.17	0.20	72.3 (499)	0.8 (6)	6 (41)	9229	+0.96	1
1044	1.1 (7.6)	0	0.50	0.18	0.20	71.3 (492)	0.4 (3)	6 (41)	13474	+1.61	10
1024	1.1 (7.6)	1C	0.50	0.16	0.18	78.2 (539)	1.2 (8)	6 (41)	5069[c]	+1.18	-
1049	1.1 (7.6)	1C	0.50	0.17	0.20	75.9 (523)	1.9 (13)	6 (41)	8283	+1.98	1
1038	1.1 (7.6)	1T	0.50	0.16	0.17	76.8 (530)	0.1 (1)	6 (41)	3821	+1.21	1
1041	1.1 (7.6)	1T	0.50	0.17	0.18	74.8 (516)	0.2 (1)	6 (41)	2746	+1.04	20
1098[d]	2.0 (13.8)	0	0.50	0.19	0.19	83.7 (577)	4.2 (29)	11 (76)	61514	+0.62	-
1059	2.0 (13.8)	0	0.50	0.15	0.19	77.4 (534)	-0.1 (-1)	11 (76)	14583[b]	+3.15	-
1050	2.0 (13.8)	1C	0.50	0.13	0.20	84.2 (581)	1.6 (11)	11 (76)	7140[b]	+4.67	-

[a] T and C denote tensile and compressive hold, respectively.

[b] Specimen failed outside gauge section.

[c] Specimen failed at thermocouple.

[d] Specimen tested at room temperature at a strain rate of 10^{-3}/s.

Table IV. Summary of Biaxial Creep-fatigue Tests for Incoloy 800 (Axial Strain Rate = 10^{-3}/s)

Test No.	Internal Pressure, ksi (MPa)	Hold[a] Time, min	Axial Strain Range, %		Diam Strain Range, %	Axial Stress, ksi (MPa)		Hoop Stress, ksi (MPa)	Cycles to Failure	Mean Diam Strain at Failure, %	No. of Initiation Sites
			Total	Plastic		Range	Mean				
1053[b]	0	0	0.50	0.21	0.19	64.8 (447)	1.6 (11)	0	33498	-0.02	1
1064	0	0	0.49	0.20	0.19	64.5 (451)	-0.3 (-2)	0	6355	-0.10	11
1067	0	0	0.50	0.20	0.20	66.5 (459)	-0.5 (-3)	0	22438	-0.05	6-7
1062	0	1C	0.49	0.19	0.20	68.2 (471)	0.6 (4)	0	4273	-0.11	15
1068	0	1C	0.49	0.18	0.19	69.5 (479)	0.9 (6)	0	11561	-0.08	4-6
1070	0	1C	0.50	0.19	0.18	69.4 (478)	1.8 (12)	0	17254	-0.07	1
1066	0	1T	0.50	0.18	0.20	66.7 (460)	-0.5 (-3)	0	11142	-0.07	1
1069	0	1T	0.50	0.18	0.19	70.9 (489)	-1.9 (-13)	0	13791	-0.05	1
1057[b]	1.1 (7.6)	0	0.51	0.20	0.21	68.1 (470)	2.3 (17)	6 (41)	9359	+1.17	11
1091	1.1 (7.6)	0	0.49	0.17	0.21	70.0 (483)	0.9 (6)	6 (41)	27440	+1.48	1
1073	1.1 (7.6)	1C	0.50	0.18	0.20	70.2 (484)	3.2 (22)	6 (41)	6903	+1.65	8
1079	1.1 (7.6)	1C	0.50	0.18	0.20	71.2 (491)	3.9 (27)	6 (41)	12394	+1.71	4-6
1075	1.1 (7.6)	1T	0.50	0.17	0.22	72.2 (497)	0.8 (6)	6 (41)	17236	+1.65	1
1061[b]	2.0 (13.8)	0	0.51	0.18	0.23	72.8 (502)	3.6 (25)	11 (75)	9047	+3.44	6-7
1092	2.0 (13.8)	0	0.48	0.15	0.23	73.4 (506)	1.0 (7)	11 (75)	17315	+3.70	1
1082	2.0 (13.8)	1C	0.50	0.16	0.24	75.3 (519)	5.8 (40)	11 (75)	5245	+6.06	1
1087	2.0 (13.8)	1C	0.51	0.17	0.24	75.1 (518)	2.0 (14)	11 (75)	8686	+5.08	1

[a] T and C denote tensile and compressive hold, respectively.

[b] These tests were run at an axial strain rate of 4×10^{-3}/s.

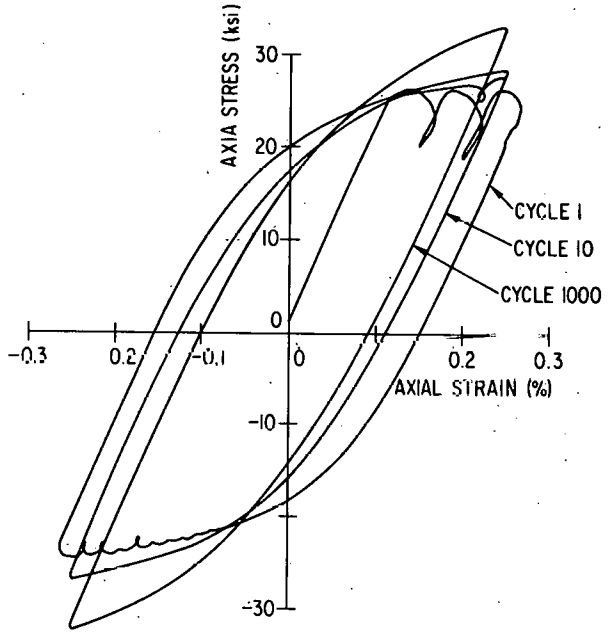

Fig. 2. Hysteresis Loops for Incoloy 800 (Test No. 1064) at an Axial Strain Rate of 1 x 10^{-3}/s at 1100°F.

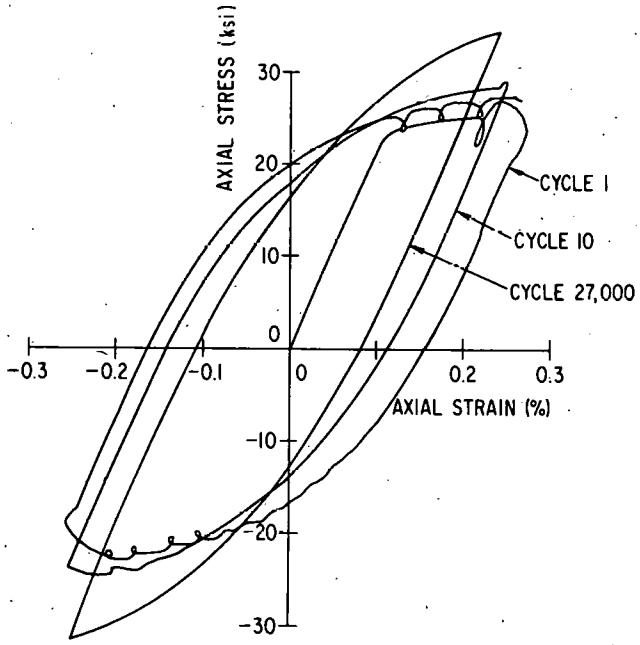

Fig. 3. Hysteresis Loops for Incoloy 800 (Test No. 1053) at an Axial Strain Rate of 4 x 10^{-3}/s at 1100°F.

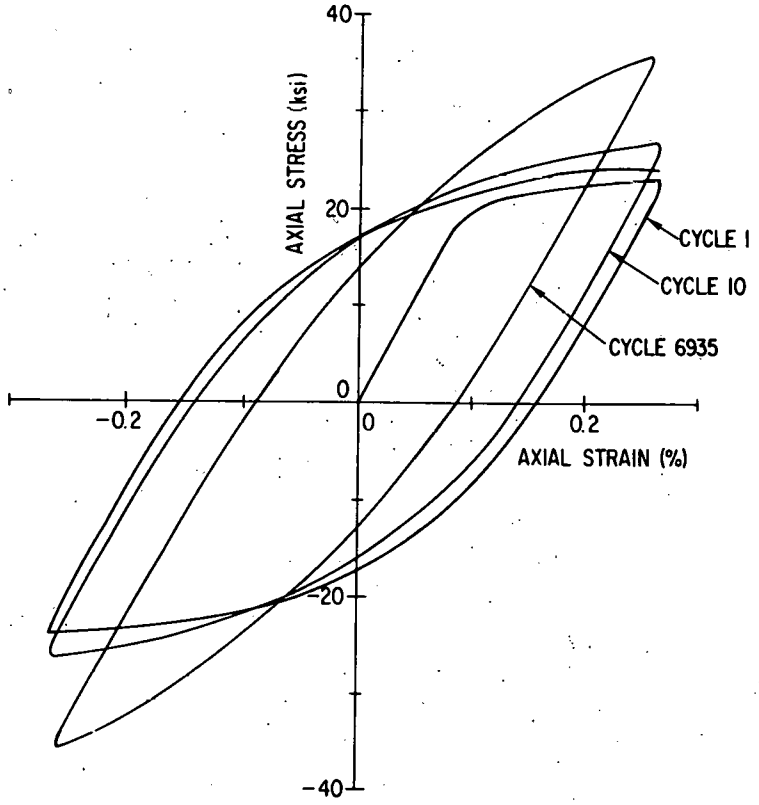

Fig. 4. Hysteresis Loops for Type 316H Stainless Steel (Test No. 997) at an Axial Strain Rate of 4 x 10^{-3}/s at 1100°F.

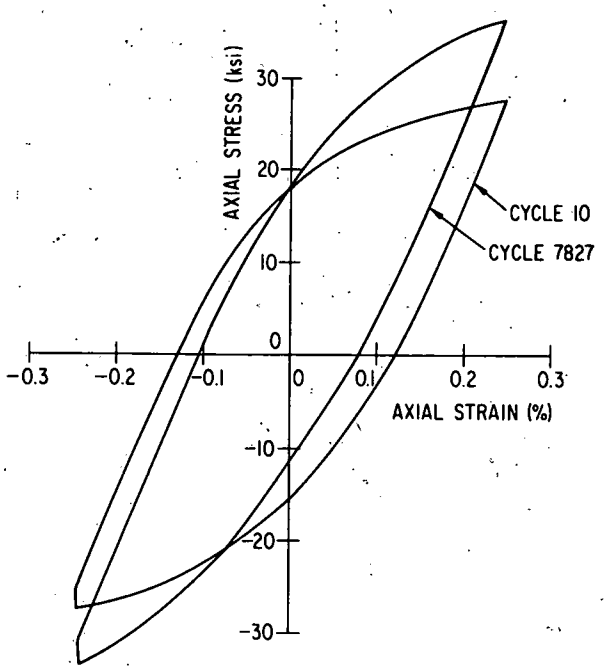

Fig. 5. Hysteresis Loops for Test 1070 (p = 0, Hold Time = 1C).

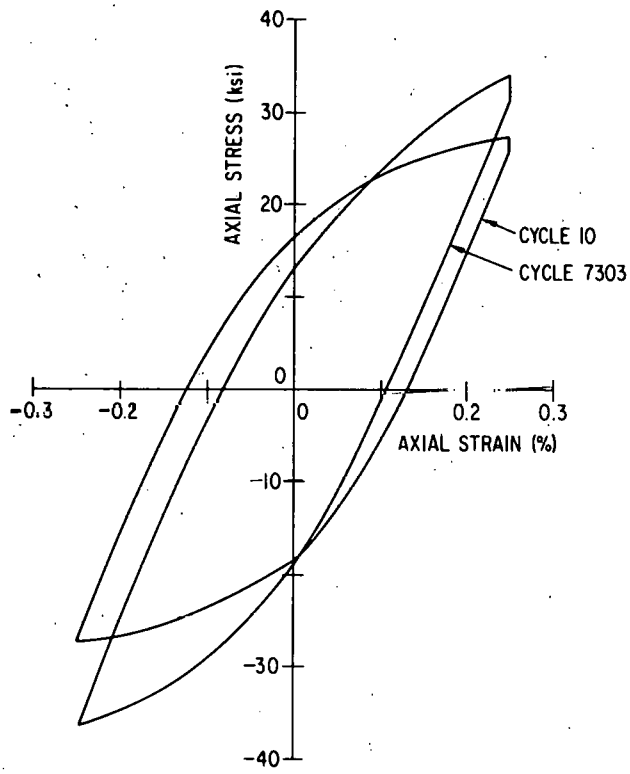

Fig. 6. Hysteresis Loops for Test 1069 (p = 0, Hold Time = 1T).

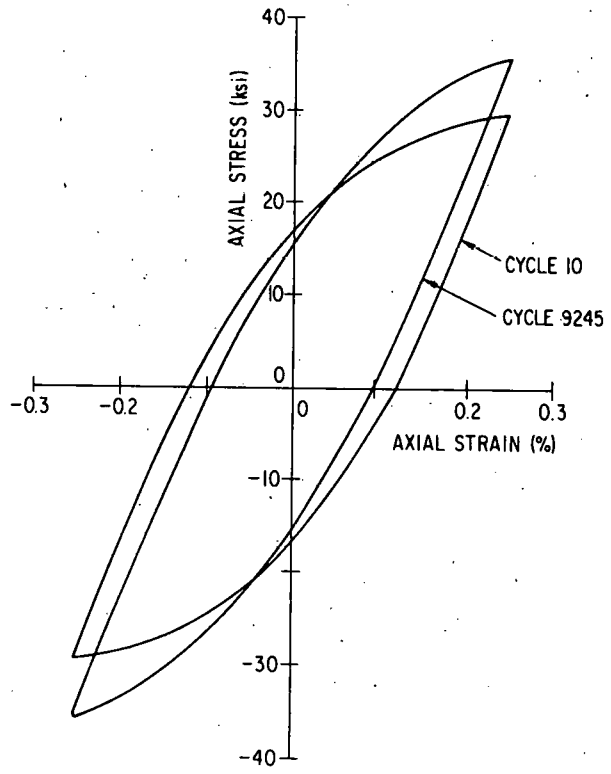

Fig. 7. Hysteresis Loops for Test 1091 (p - 1100 psi, Hold Time = 0).

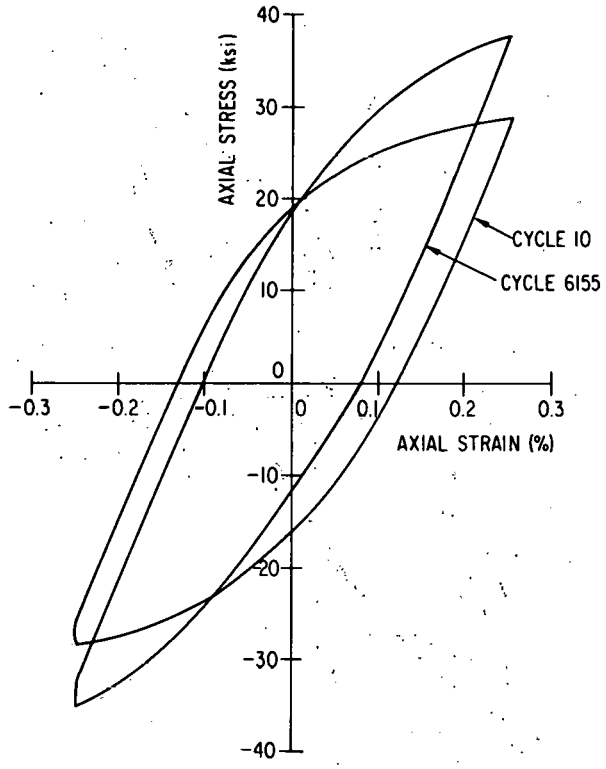

Fig. 8. Hysteresis Loops for Test 1079 (p = 1100 psi, Hold Time = 1C).

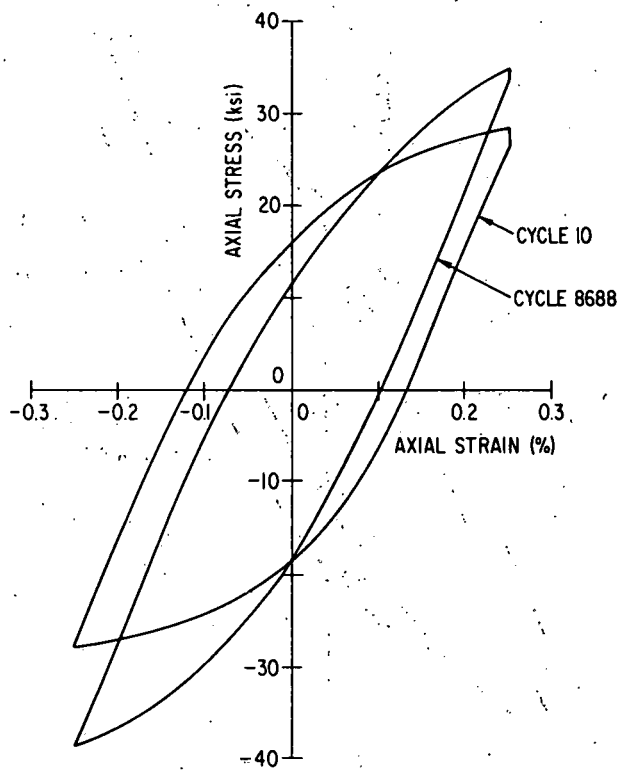

Fig. 9. Hysteresis Loops for Test 1075 (p = 1100 psi, Hold Time = 1T).

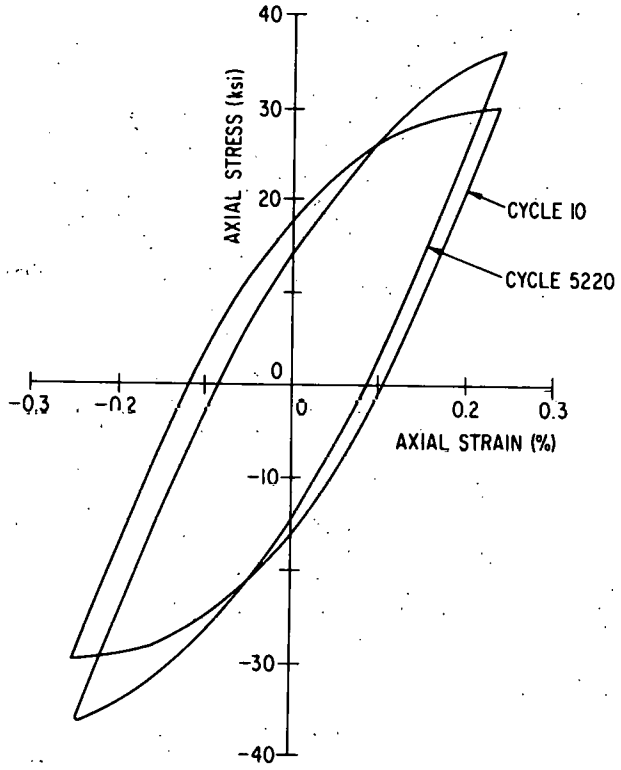

Fig. 10. Hysteresis Loops for Test 1061 (p = 2000 psi, Hold Time = 0).

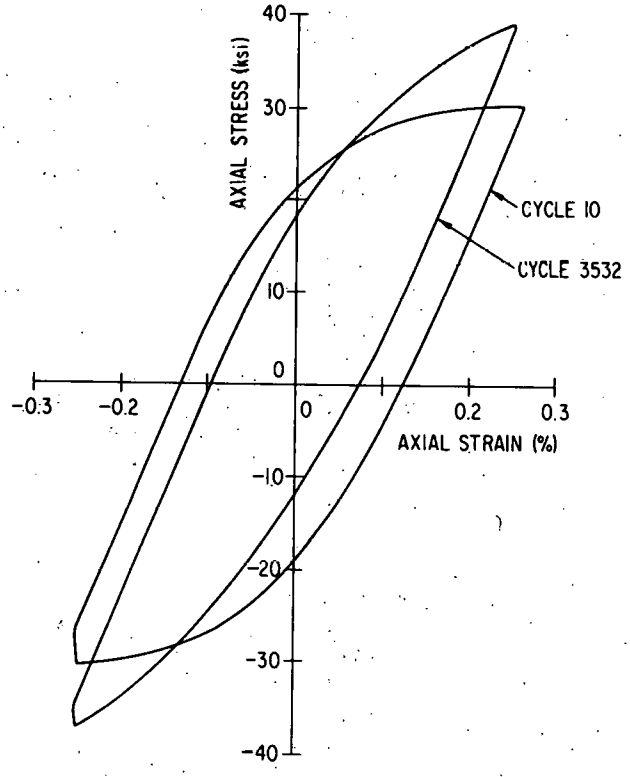

Fig. 11. Hysteresis Loops for Test 1082 (p = 2000 psi, Hold Time = 1C).

Comparable plots for Type 316 stainless steel are given in Ref. 1. Although both materials undergo significant cyclic hardening, Type 316H stainless steel tends to harden somewhat more than Incoloy 800. However, at room temperature Type 316H undergoes very little hardening, as is evident in Fig. 12. It should be borne in mind that since the cyclic hardening behavior of an alloy is sensitive to its grain size, the cyclic stress response for a finer-grained heat of Incoloy 800 may be different from that in the present program.

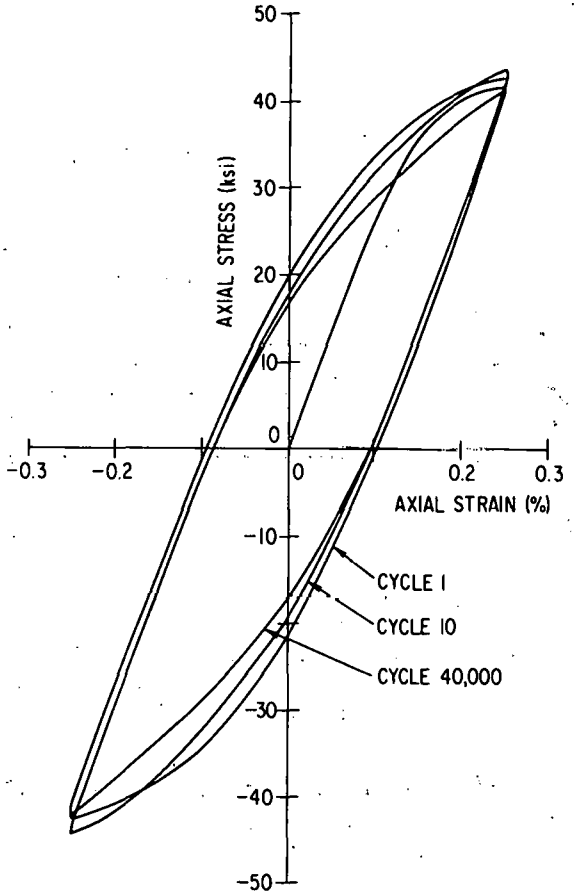

Fig. 12. Hysteresis Loops for Type 316H Stainless Steel at Room Temperature (Test 1098).

Typical stress-relaxation behavior of Incoloy 800 and Type 316H stainless steel is shown in Fig. 13. The plots include relaxation data for 1-min tensile and compressive hold tests of both pressurized and unpressurized tubes. The initial more rapid drop of stress in Type 316H stainless steel than in Incoloy 800 may be explained in terms of the difference in strain rates between the two series of tests. Type 316H stainless steel specimens, having been cycled at a faster strain rate than the Incoloy 800 specimens, experience a more rapid load drop at the beginning of the hold time because of anelasticity effects and also because there is a slightly larger overshoot in strain in the Type 316H stainless steel specimens, which were tested at a higher strain rate than the Incoloy 800 specimens.

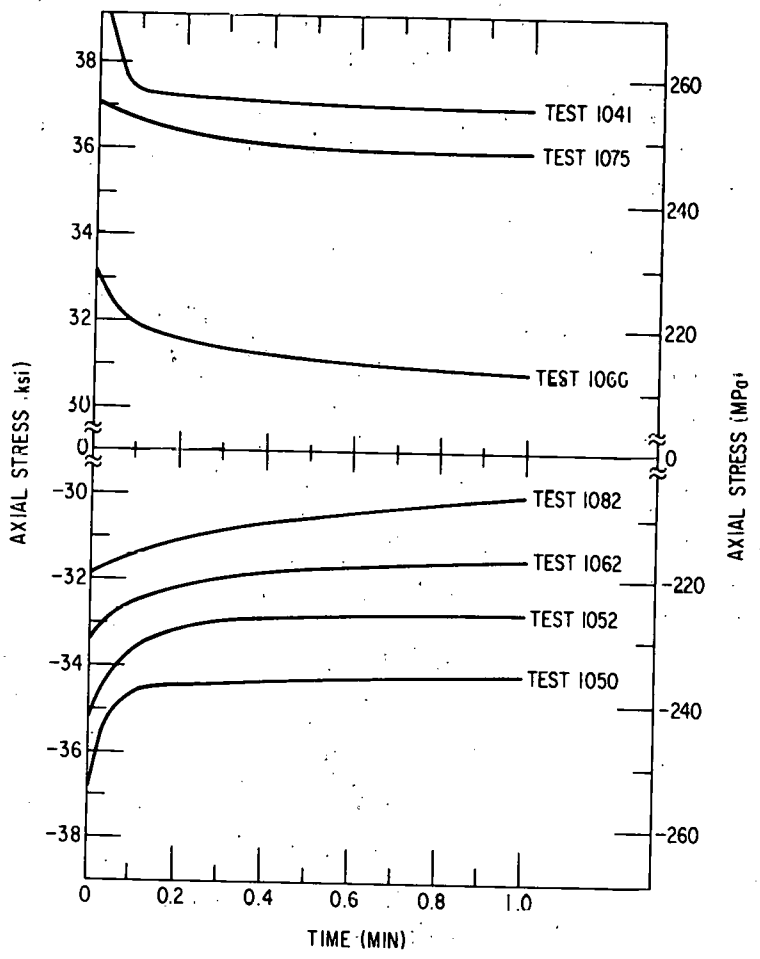

Fig. 13. Stress-relaxation Behavior of Incoloy 800 and Type 316H Stainless Steel at 1100°F.

IV. DISCUSSION

Figures 14 and 15 contain the axial hardening data for continuous-cycling fatigue of both materials without and with internal pressure, respectively. Note that in each case the hardening behavior of Type 316 stainless steel is very similar to that of Incoloy 800, with Type 316 stainless steel achieving a slightly higher stable stress range value than Incoloy 800. Note that in both materials, the higher the internal pressure, the higher the axial hardening rate. The lack of hardening in Type 316H stainless steel in the presence of 2000 psi internal pressure at room temperature (Fig. 12) indicates that some kind of aging phenomenon may be responsible for the hardening of this material at elevated temperature. It is possible that the larger diametral ratchetting occurring in specimens with higher internal pressure is partially responsible for this higher hardening rate at elevated temperature.

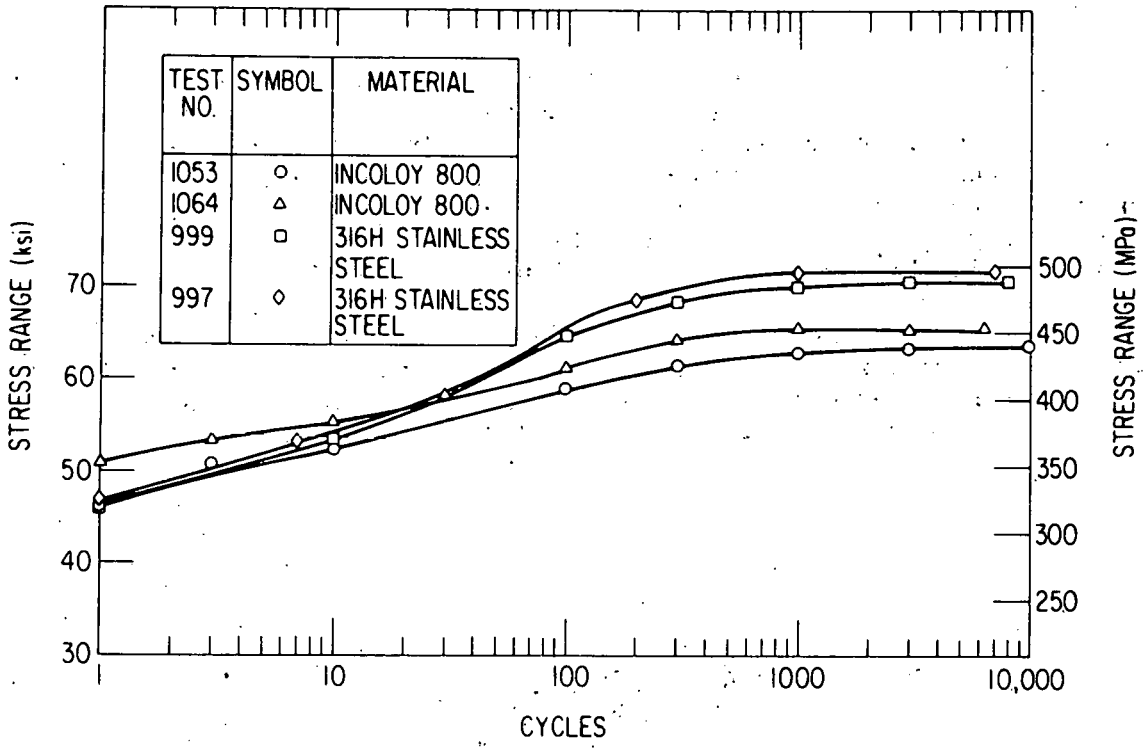

Fig. 14. Axial Stress Range Versus Cycle Plots for Continuous-cycling Fatigue with Zero Internal Pressure at 1100°F and at $\Delta\varepsilon_t$ = 0.5%.

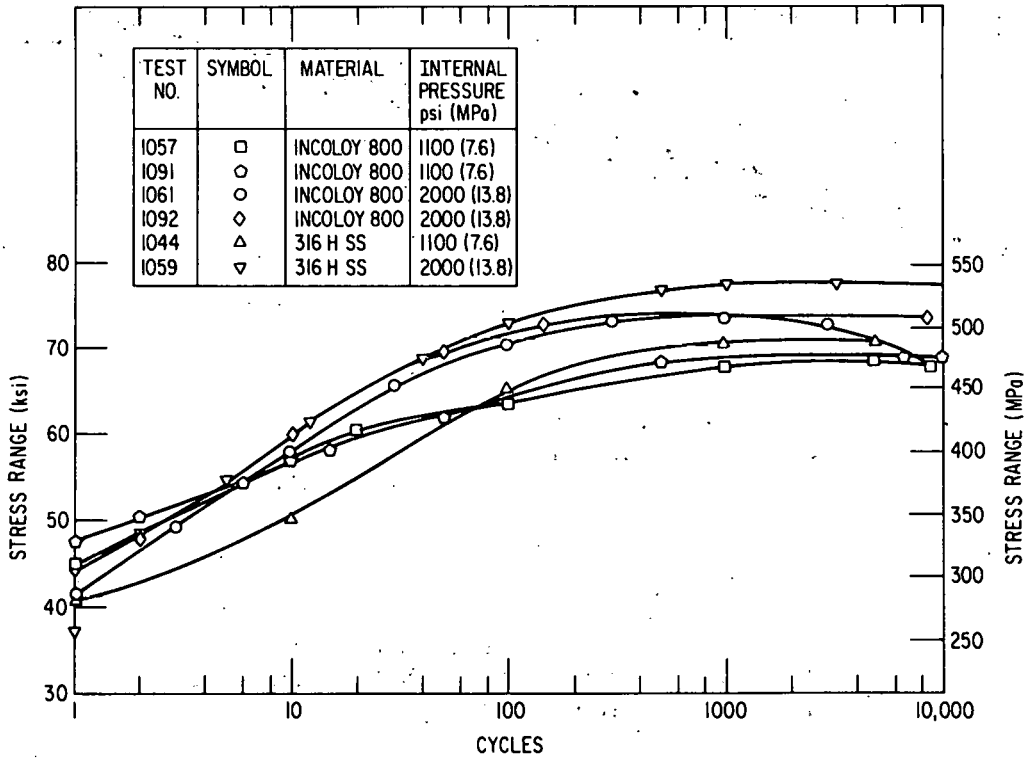

Fig. 15. Axial Stress Range Versus Cycle Plots for Continuous-cycling Fatigue with Internal Pressures at 1100°F and at $\Delta\varepsilon_t$ = 0.5%.

Axial hardening rates for both materials in the presence of compressive or tensile hold times are presented in Figs. 16-18. In contrast to continuous-cycling specimens, the specimens in most hold-time tests, both with and without internal pressure, do not achieve a stable stress range with cycling but continue to harden throughout life, often after reaching what initially appears to be a stable behavior. Note also that the final stress range in the presence of internal pressure is higher than that in the absence of internal pressure for both materials. Note again that, when subjected to the same cycle shape, Type 316H stainless steel tends to achieve a slightly higher stress range than Incoloy 800 with continued cycling even though the stress range in Type 316H stainless steel may initially be equal to or slightly less than that in Incoloy 800.

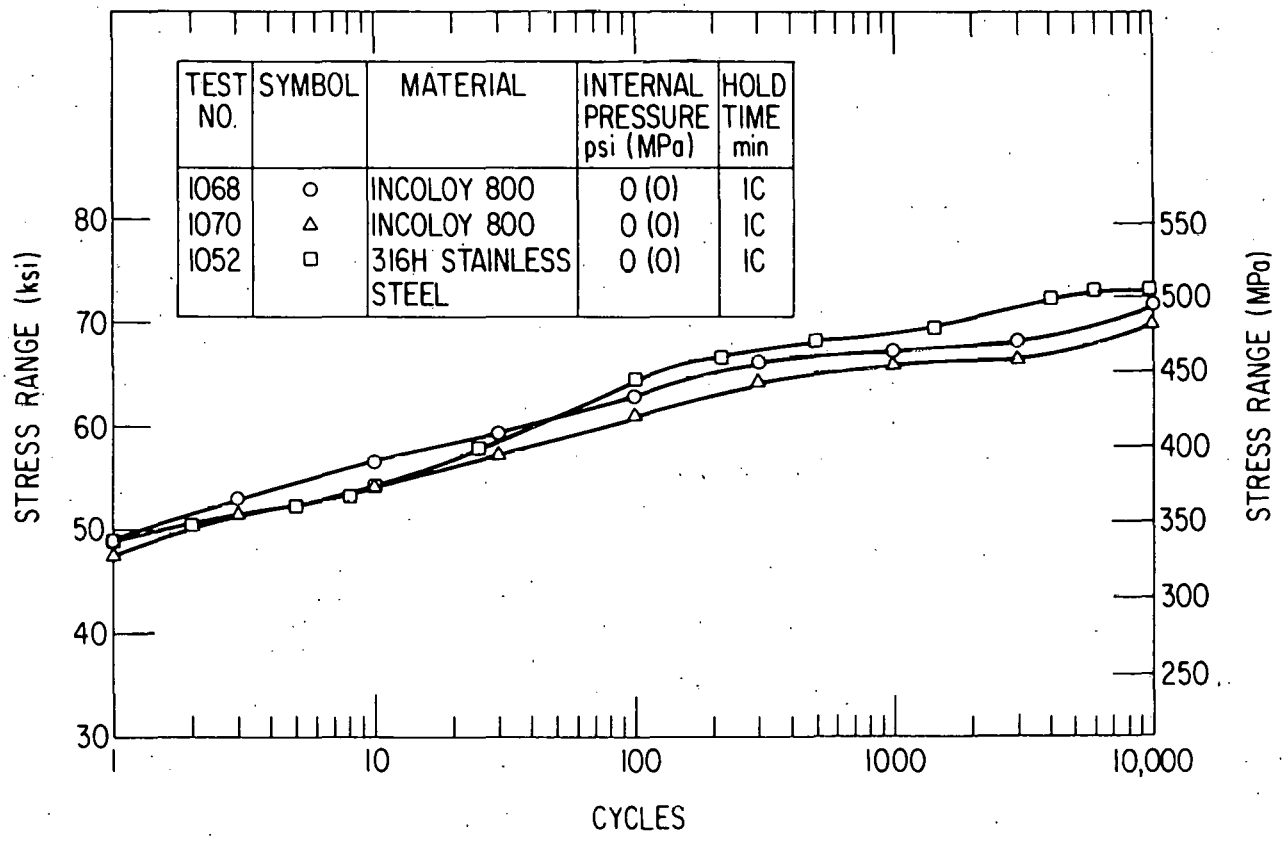

Fig. 16. Axial Stress Range Versus Cycles for 1-min Compressive Hold Tests with Zero Internal Pressure at 1100°F and $\Delta\varepsilon_t$ = 0.5%.

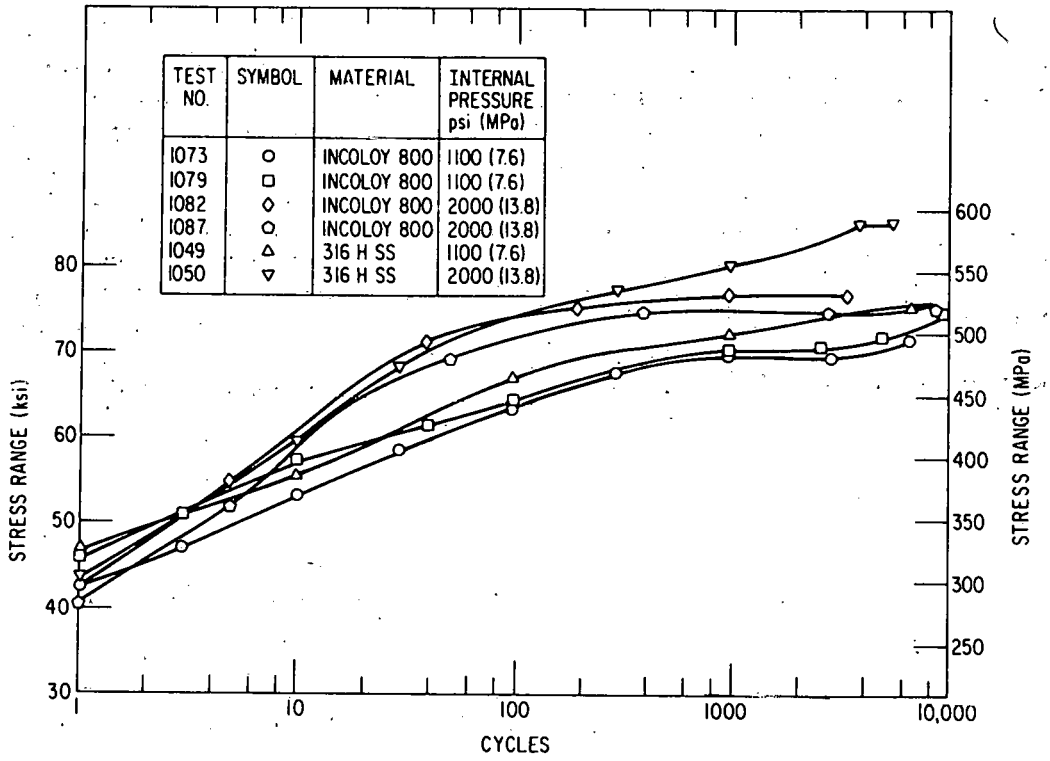

Fig. 17. Axial Stress Range Versus Cycles for 1-min Compressive Hold Tests with Internal Pressure at 1100°F and $\Delta\varepsilon_t$ = 0.5%.

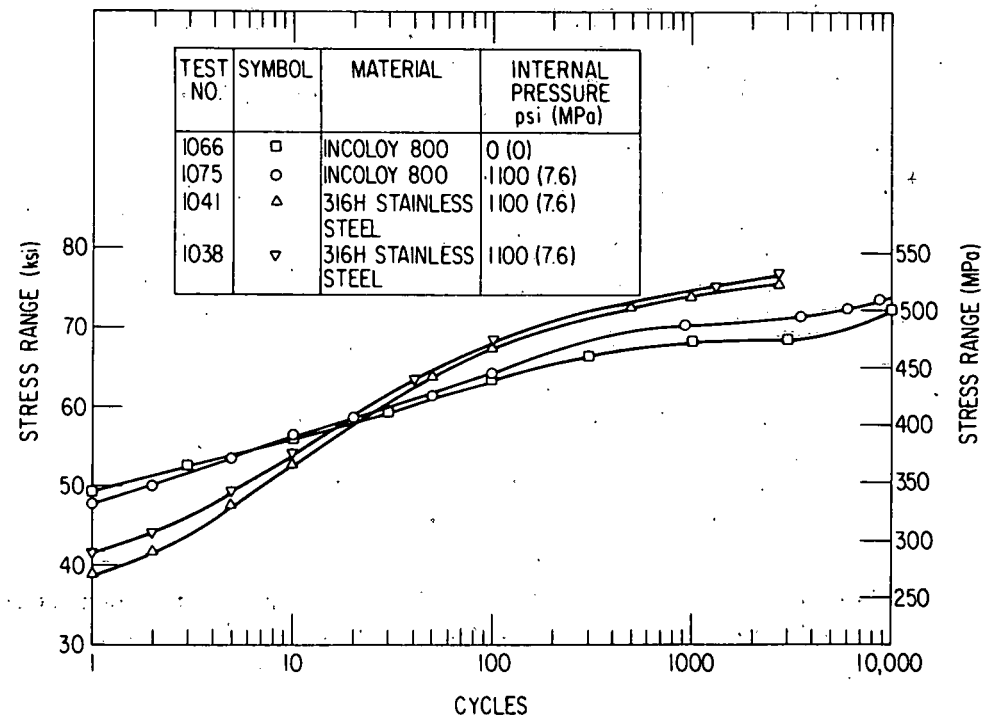

Fig. 18. Axial Stress Range Versus Cycles for 1-min Tensile Hold Tests at 1100°F and $\Delta\varepsilon_t$ = 0.5%.

Although the hysteresis loops for both materials are similar in shape under continuous cycling without hold time, they differ markedly in shape when either a 1-min tensile or compressive hold is imposed on the cycle. For example, Fig. 19 shows the hysteresis loops at half-life for Type 316H stainless steel undergoing hold time in tension and compression. Note that the tension-going half of the hysteresis loop of the tensile-hold test and the compression-going half of the hysteresis loop of the compressive-hold test are almost bilinear in shape, whereas the remaining halves of the hysteresis loops are rounded as usual. This asymmetry in loop shape is not present at the beginning of the test but develops as the material hardens. Incoloy 800, on the other hand, does not develop such an asymmetric hysteresis-loop shape when subjected to similar hold-time cycles (Figs. 8-9).

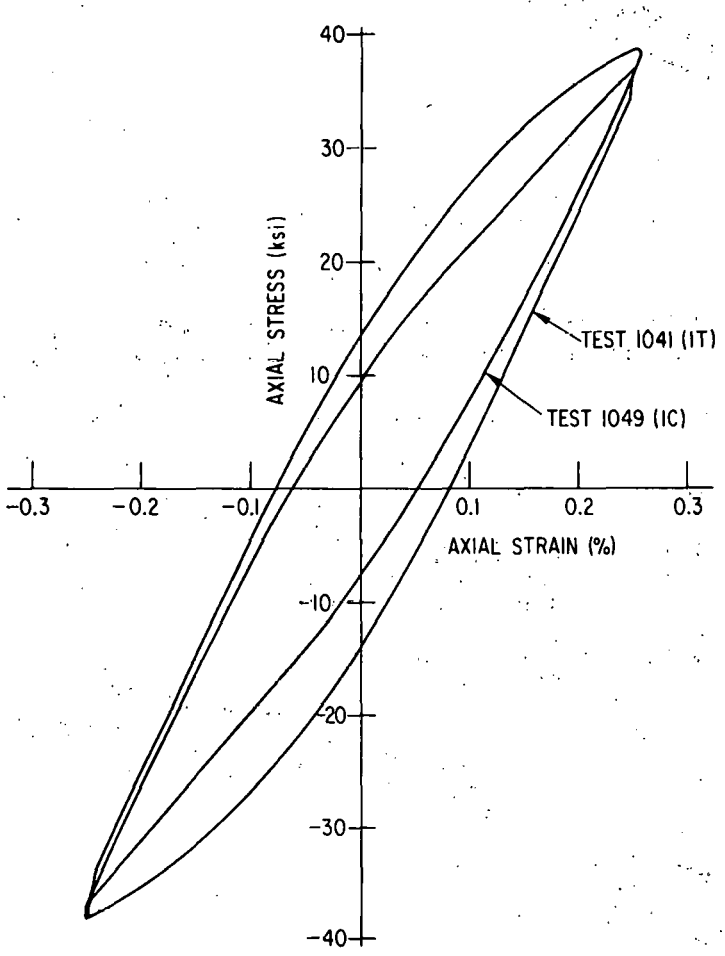

Fig. 19. Hysteresis Loops for 1-min Tensile Hold and 1-min Compressive Hold Tests of Type 316H Stainless Steel at 1100°F.

The stress-relaxation parameters for Incoloy 800 and Type 316H stainless steel at half-life are given in Tables V and VI, respectively. In general, the stress at the beginning of the hold and the amount of stress relaxation during hold are larger in Type 316H stainless steel than in Incoloy 800. This difference in behavior is partly due to the fact that the Type 316H stainless steel specimens were cycled at 4×10^{-3}/s whereas the Incoloy 800 specimens were cycled at 10^{-3}/s. The hold times and the stress-biaxiality ratios in the present tests are too small to show conclusively the effect of the stress biaxiality on the stress-relaxation behavior. However, the unpressurized Incoloy 800 specimens tend to show a somewhat larger stress relaxation than the pressurized specimens--a trend which is not evident in the Type 316H stainless steel specimens. Tests with larger biaxiality in stress and longer hold times are needed to fully explore the effects of stress biaxiality on the stress-relaxation behavior.

Table V. Summary of Relaxation of Stresses at Half-life for the 1-min Hold-time Tests on Incoloy 800 at 593°C (1100°F) and $\Delta\varepsilon_t = 0.5\%$

Test No.	Hold Time, min	Maximum Hoop Stress, ksi (MPa)	Axial Tensile Stress During Hold, ksi (MPa)		Axial Compressive Stress During Hold, ksi (MPa)	
			Beginning	End	Beginning	End
1062	1C	0 (0)	34.8 (240)	-	33.4 (230)	31.5 (217)
1068	1C	0 (0)	35.4 (244)	-	34.1 (235)	31.8 (219)
1070	1C	0 (0)	36.8 (254)	-	32.6 (225)	30.7 (212)
1073	1C	6.0 (41)	38.6 (266)	-	31.6 (218)	30.0 (207)
1079	1C	6.0 (41)	39.7 (274)	-	31.5 (217)	30.1 (208)
1082	1C	11.0 (76)	43.5 (300)	-	31.8 (219)	30.0 (207)
1087	1C	11.0 (76)	43.3 (299)	-	31.8 (219)	30.3 (209)
1066	1T	0 (0)	33.2 (229)	30.9 (213)	33.5 (231)	-
1069	1T	0 (0)	33.4 (230)	31.1 (214)	37.5 (259)	-
1075	1T	6.0 (41)	37.1 (256)	36.0 (248)	35.1 (242)	-

Table VI. Summary of Relaxation of Stresses at Half-life for the 1-min Hold-time Tests on Type 316H Stainless Steel at 593°C (1100°F) and $\Delta\varepsilon_t = 0.5\%$

Test No.	Hold Time, min	Average Hoop Stress, ksi (MPa)	Axial Tensile Stress During Hold, ksi (MPa)		Axial Compressive Stress During Hold, ksi (MPa)	
			Beginning	End	Beginning	End
1035	1C	0	38.7 (267)	-	36.4 (251)	34.6 (239)
1052	1C	0	38.7 (267)	-	35.3 (243)	32.7 (225)
1024	1C	6.0 (41)	40.3 (278)	-	37.9 (261)	35.7 (246)
1049	1C	6.0 (41)	39.9 (275)	-	36.0 (248)	33.6 (232)
1050	1C	11.0 (76)	43.7 (301)	-	40.5 (279)	37.8 (261)
1038	1T	6.0 (41)	38.5 (265)	35.9 (248)	38.3 (264)	-
1041	1T	6.0 (41)	37.6 (259)	35.1 (242)	37.2 (256)	-

The diametral ratchetting under internal pressure for continuous-cycling, 1-min compressive hold, and 1-min tensile hold tests are shown in Figs. 20, 21 and 22, respectively. At 1100 psi internal pressure (hoop stress = 6 ksi) under cycling with no hold time, Type 316H stainless steel undergoes slightly larger diametral ratchetting than Incoloy 800, but at 2000 psi (hoop stress = 11 ksi) the trend is reversed. At room temperature, Type 316H stainless steel under 2000 psi internal pressure undergoes far less diametral ratchetting than at 1100°F, indicating that the larger-diametral ratchetting at elevated temperature is attributable to thermally activated creep. Note, however, that even at room temperature the diametral ratchetting in Type 316H stainless steel occurs at a slower and slower rate with cycles but never quite reaches a zero rate of ratchetting. At an internal pressure of 1100 psi (hoop stress = 6 ksi), both materials undergo similar diametral ratchetting when subjected to either 1-min tensile hold or 1-min compressive hold cycling. Furthermore, the ratchetting behavior under tensile hold cycling is similar to that under compressive hold cycling, with both hold cycles resulting in larger diametral ratchetting than in cycles without hold. However, at an internal pressure of 2000 psi (hoop stress = 11 ksi), Incoloy 800 undergoes slightly greater diametral ratchetting than Type 316H stainless steel when subjected to 1-min compressive hold cycling.

From a comparison of the cycles to failure in Tables III and IV it is evident that the data for Incoloy 800 showed much greater scatter than that for Type 316H stainless steel. An examination of the last column in Table IV shows that the number of cycles to failure varies inversely with the number of initiation sites for the Incoloy 800 specimens. For example, test 1053 (which lasted 33498 cycles) had a single initiation site, whereas test 1064 (which lasted 6355 cycles) had 11 initiation sites (Fig. 23). This

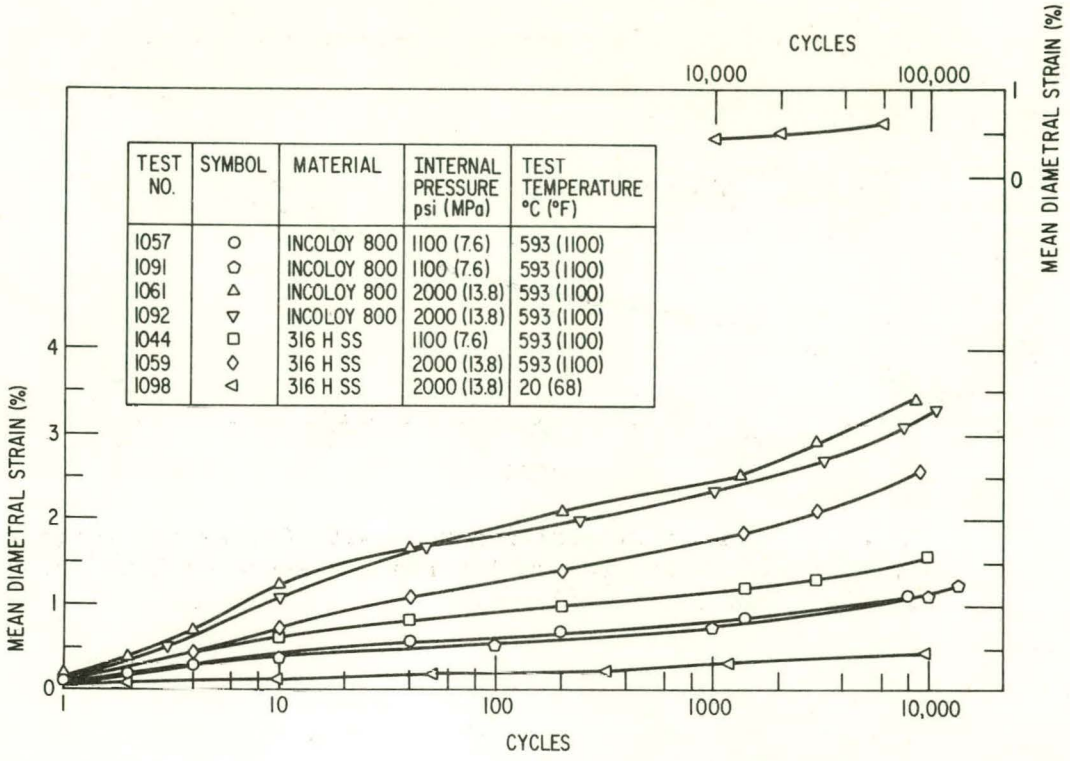

Fig. 20. Variation of Mean Diametral Strain with Cycles for Continuous-cycling Fatigue with Internal Pressure at 1100°F and $\Delta\varepsilon_t$ = 0.5%.

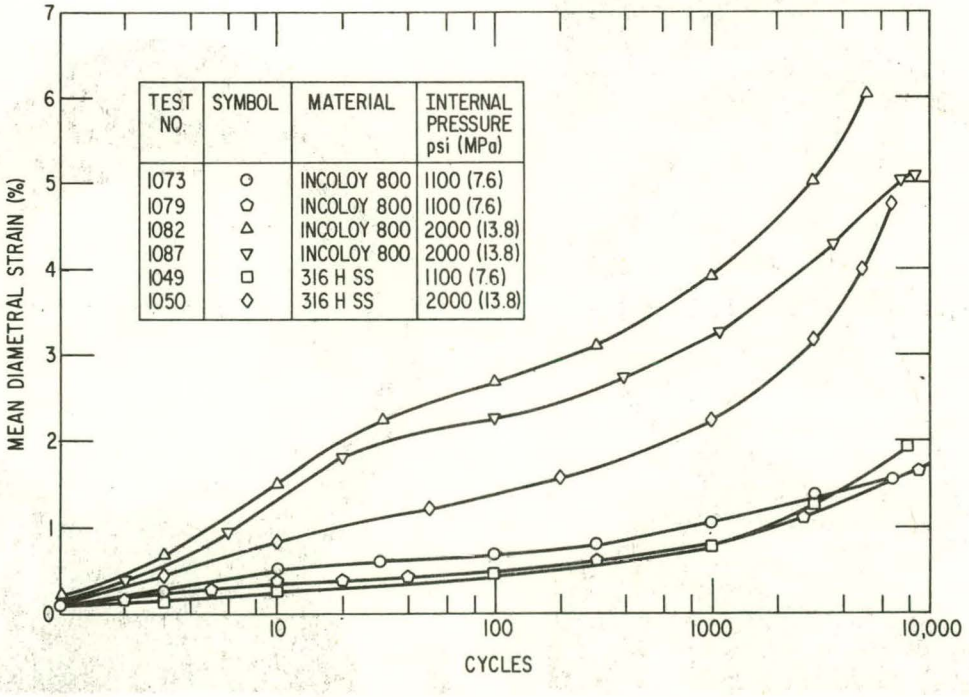

Fig. 21. Variation of Mean Diametral Strain with Cycles for 1-min Compressive Hold-time Tests with Internal Pressure at 1100°F and $\Delta\varepsilon_t$ = 0.5%.

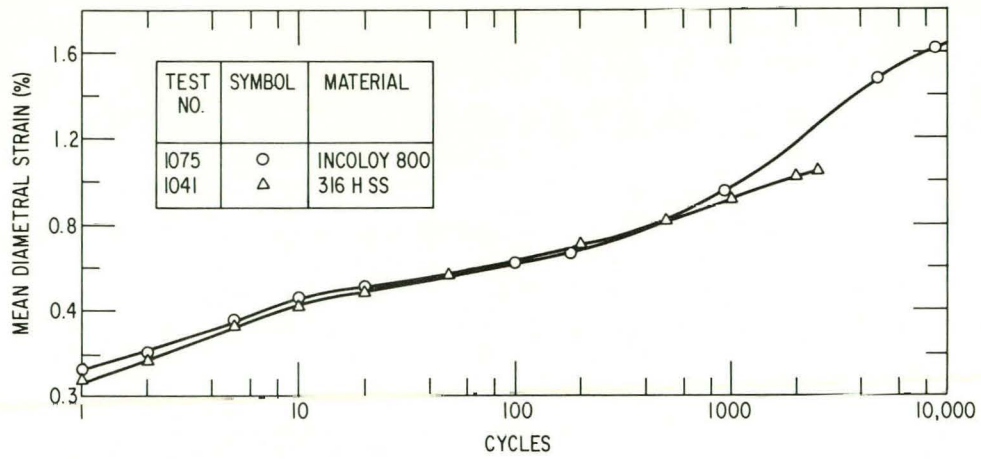

Fig. 22. Variation of Mean Diametral Strain with Cycles for 1-min Tensile-hold Tests with an Internal Pressure of 1100 psi at 1100°F and $\Delta\varepsilon_t$ = 0.5%.

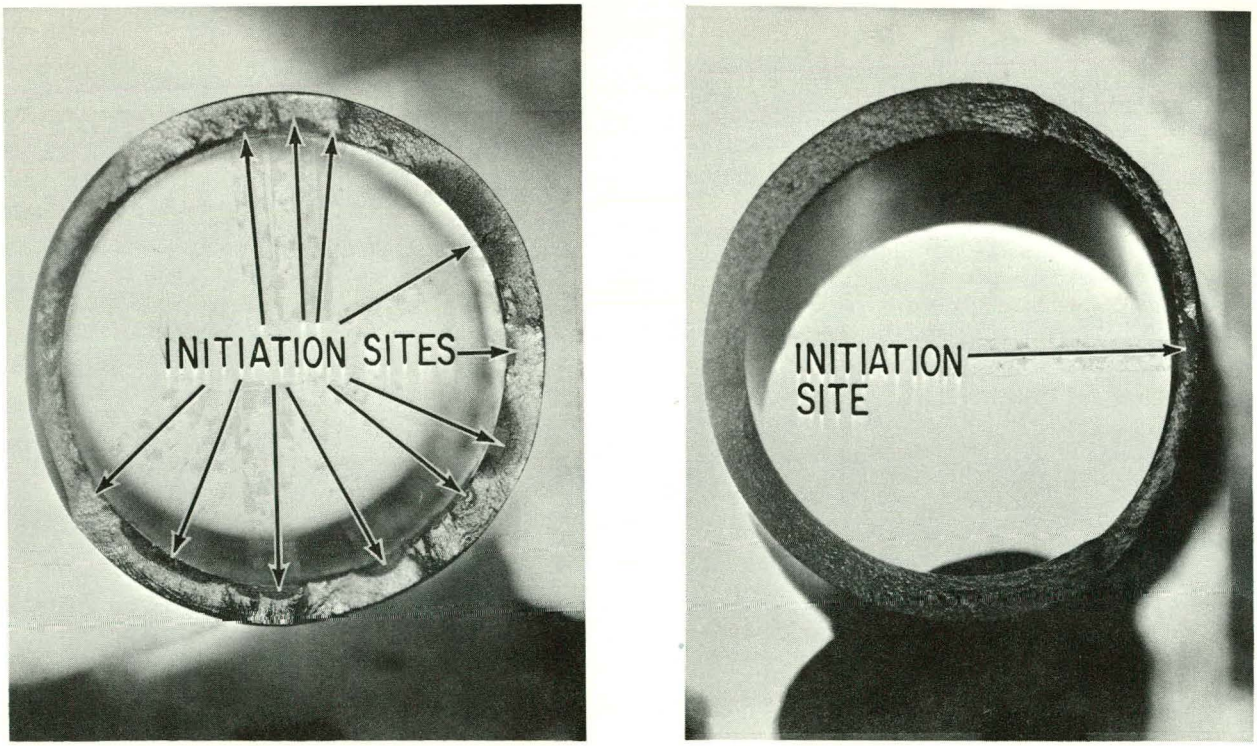

Fig. 23. Number of Initiation Sites for Incoloy 800 Specimens under Continuous-cycling Fatigue at 1100°F (593°C).

negative correlation between number of initiation sites and cycles to failure is not observed in Type 316H stainless steel (compare tests 1001, 1012, 1044 in Table III). It is interesting to note that in uniaxial solid specimens of Incoloy 800 (from a different heat) the number of cycles to failure is found to be independent of the number of initiation sites.[2] Thus, the observed anomalous behavior in cyclic life may be unique to the heat of Incoloy 800 tested in the present program. To further investigate the reason for this anomalous behavior, fracture surfaces from tests 1053 and 1064 were examined in a scanning electron microscope (Fig. 24). It was observed that at the inner-diameter surface of the specimen from test 1064, which had the shortest life, the grain boundaries were delineated as if they were etched and the fracture was intergranular near the initiation sites. The specimen from test 1053, which had the longest life, did not exhibit such delineated grain boundaries at the inner-diameter surface. A similar contrast was also observed for tests 1062 and 1070. A chemical wet analysis of samples taken from the fracture surfaces of tests 1053 and 1064 (Table I), however, did not reveal any significant difference in composition between the two specimens.

An examination of Tables III and IV shows that the continuous-cycling fatigue life of both materials at an axial strain range of 0.5% is not affected significantly by the imposition of a steady internal pressure of 2000 psi (hoop stress = 11 ksi) at a temperature of 1100°F. In Type 316H stainless steel, a 1-min tensile hold is much more damaging than a compressive hold time of equal duration even under a biaxial state of stress. The reason for the short life under tensile hold is the predominantly intergranular fracture of Type 316H stainless steel specimens, as shown in Fig. 25. Under continuous cycling or with 1-min compressive hold the fracture is transgranular with striations on the fracture surface. In Incoloy 800, on the other hand, both 1-min tensile hold and 1-min compressive hold cause very little reduction in life as compared with continuous cycling for tests carried out with zero or 1100 psi internal pressure. In contrast to Type 316H stainless steel, Incoloy 800 specimens in 1-min tensile hold tests show predominantly transgranular fracture (with striations), although some isolated patches of intergranular fracture are present near the initiation site (Figs. 26-27). A 1-min compressive hold per cycle with 2000 psi internal pressure (hoop stress = 11 ksi) causes some reduction in the fatigue life of Incoloy 800, which may in part be attributable to the larger-diametral ratchetting incurred in these tests.

It is interesting to compare the fatigue lives of Type 316H stainless steel and Incoloy 800 obtained in the present program with those reported in the literature. The continuous-cycling fatigue life of Type 316 stainless steel when cycled uniaxially at 0.5% strain range at 1100°F varies from 10780 to 106622 cycles, depending on the heat of material.[3] The tensile-hold fatigue life for Type 316 stainless steel at 0.5% varies from 8400-21600 cycles for a 0.6-min hold to 1985 cycles for a 6-min hold. There are no data available for compressive hold at 0.5% strain range. The continuous-cycling fatigue life for Incoloy 800H when cycled uniaxially at 0.5% strain range at 1100°F shows a large scatter and varies from 20611 to 7×10^5, depending on the heat of material.[4] Creep-fatigue data for Incoloy 800 are rarely reported in the literature. Considering the differing

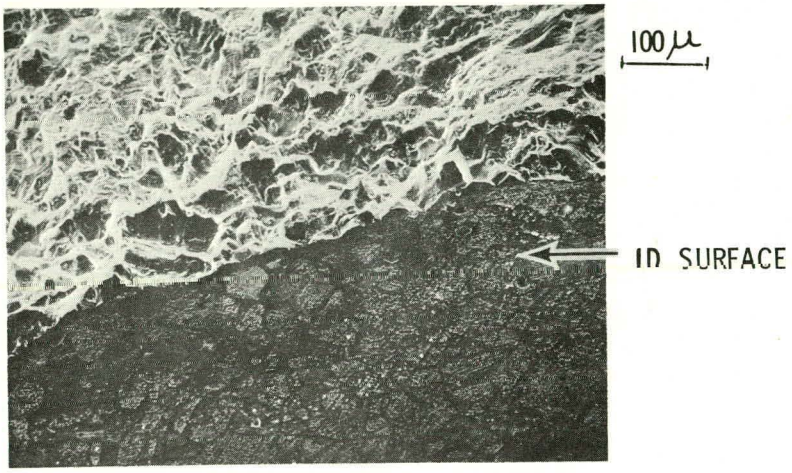

(a) TEST 1064

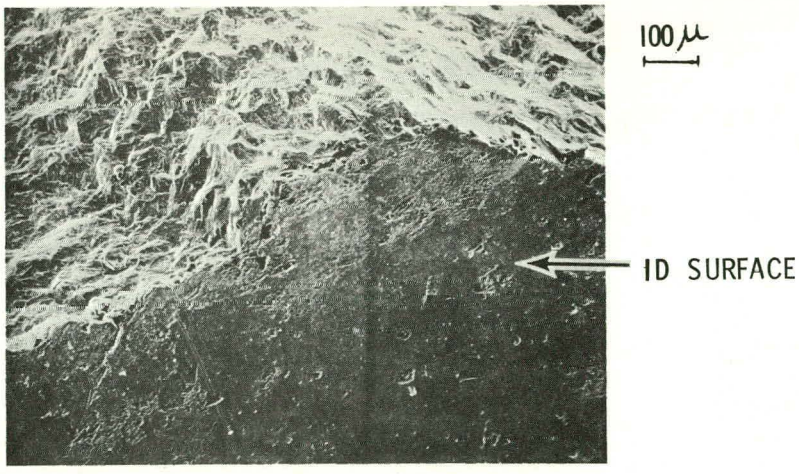

(b) TEST 1053

Fig. 24. Scanning Electron Micrographs Showing Fracture and ID Surfaces of Incoloy 800 specimens from Two Biaxial Creep-fatigue Tests.

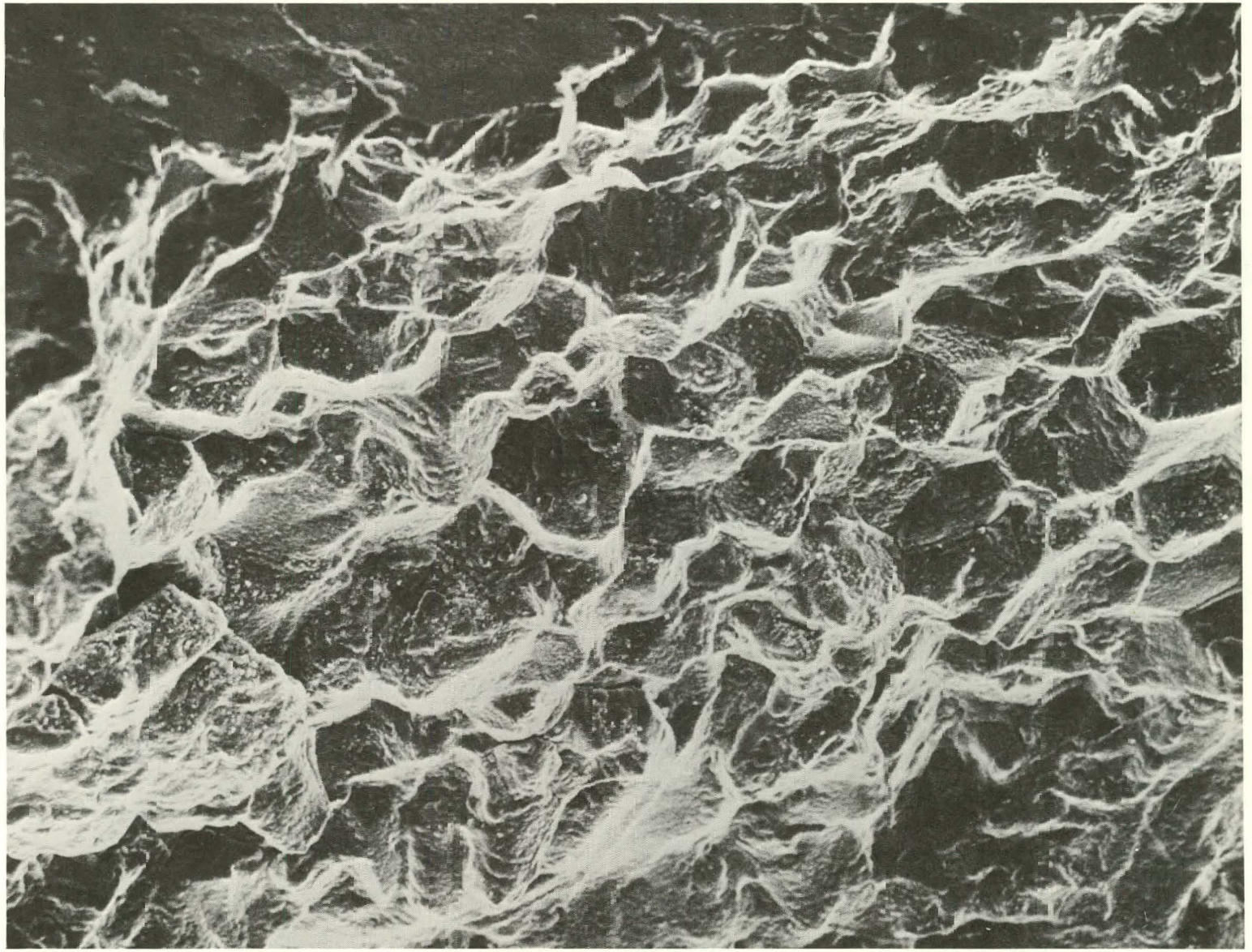

Fig. 25. Scanning Electron Micrograph of Fracture Surface from Test No. 1041.

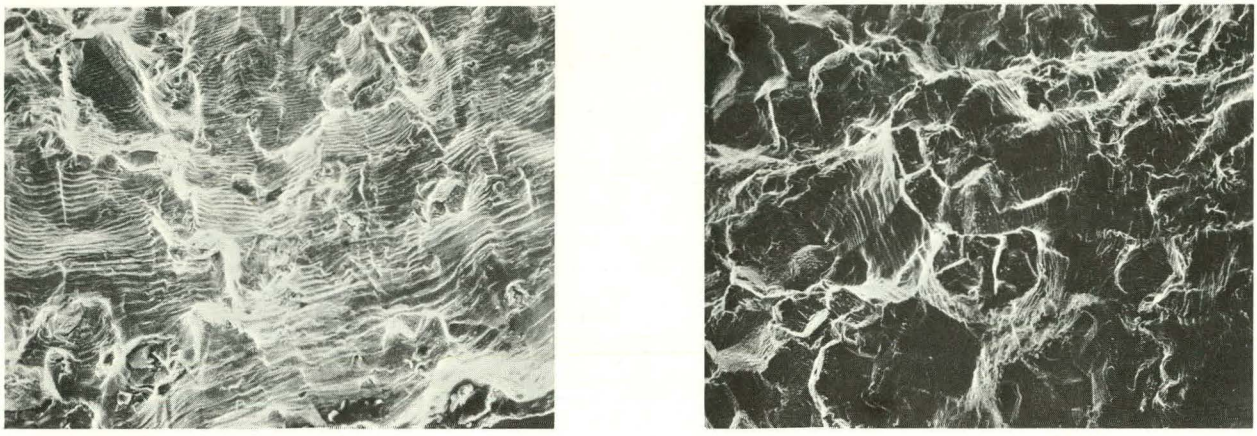

Fig. 26. Scanning Electron Micrographs of the Fracture Surface of an Incoloy 800 Specimen Subjected to 1-min Tensile Hold in Test 1066.

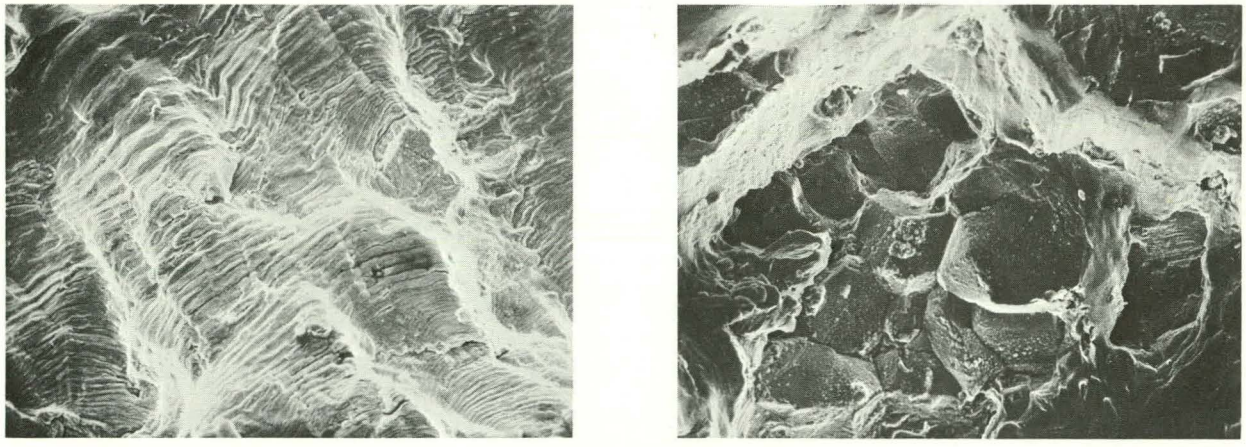

Fig. 27. Scanning Electron Micrographs of the Fracture Surface of an Incoloy 800 Specimen Subjected to 1-min Tensile Hold in Test 1069.

geometry tested in the present program, the uniaxial data obtained are well within the scatter band of the results reported in the literature.

V. CONCLUSIONS

1. The heats of Type 316H stainless steel and Incoloy 800 tested in the present program show similar cyclic stress and deformation behavior. The grain size of the Incoloy 800 material tested is rather large compared to that of an average heat of the material. Hence the results obtained for Incoloy 800 in the present program may not be applicable to a heat with smaller grain size.

2. Both materials undergo significant cyclic hardening when cycled at an axial strain range of 0.5% at elevated temperature, with Type 316H stainless steel usually achieving a slightly larger stress range than Incoloy 800 even though the stress range in Type 316H stainless steel is initially equal to or smaller than that in Incoloy 800. The rate of hardening and the final stable stress range in both materials, in the absence of hold times, increases with increasing internal pressure. When a 1-min tensile or compressive hold time is imposed, either with or without internal pressure, both materials harden more than in the absence of hold time, and in many cases cyclic hardening continues until the end of the test albeit at a slower and slower rate. Type 316H stainless steel does not harden significantly at room temperature when cycled axially without hold time at a strain range of 0.5% with a steady hoop stress of 11 ksi.

3. The hysteresis-loop shapes of both materials are similar for continuous-cycling fatigue at 1100°F. However, in the presence of a 1-min tensile or compressive hold, Type 316H stainless steel exhibits an asymmetry in the hysteresis-loop shape while Incoloy 800 does not. In a 1-min tensile hold test of Type 316H stainless steel that has been hardened, the tension-going half of the hysteresis loop is bilinear and the compression-going half is rounded as usual, and vice versa in a 1-min compressive hold test.

4. The axial stress-relaxation behavior is not significantly altered in the presence of a relatively small and steady hoop stress. However, the unpressurized Incoloy 800 specimens tend to show a somewhat larger amount of stress relaxation during hold than the pressurized specimens even though the initial stress at the beginning of hold is smaller in the former case. This trend was not observed for Type 316H stainless steel. Tests with larger biaxiality in stress and longer hold times are needed to clarify the effect of stress biaxiality on stress-relaxation behavior.

5. Both materials undergo significant diametral ratchetting when cycled in the presence of internal pressure at elevated temperature. Most of this ratchetting is due to thermally activated creep. However, Type 316H stainless steel shows some ratchetting even at room temperature. The higher the internal pressure and the longer the hold time (both tensile and compressive), the greater is the diametral ratchetting at elevated temperature.

At small values of hoop stress (6 ksi), the diametral ratchetting in Type 316H stainless steel is equal to or slightly greater than that in Incoloy 800. At higher values of hoop stress (11 ksi), the trend is reversed.

6. Both materials show little or no reduction in continuous-cycling fatigue life when internal pressure is introduced. However, the present heat of Incoloy 800 shows significant scatter in fatigue life. The source of this scatter could not be determined by either microstructural observation of the fracture surfaces or wet chemical analysis of specimens taken from the fracture surfaces. The fatigue life is found to vary inversely with the number of initiation sites. Such a negative correlation between fatigue life and number of initiation sites does not hold good for Type 316H stainless steel. The continuous-cycling fatigue life of Type 316H stainless steel at room temperature with a constant hoop stress of 11 ksi ($\Delta\varepsilon_t$ = 0.5%) is four times that at 1100°F.

7. Both materials show little reduction in fatigue life when a 1-min compressive hold is imposed. The fracture for both materials is transgranular in this case. However, for Incoloy 800 the reduction in fatigue life with 1-min compressive hold tends to become larger as the internal pressure increases. The fatigue life of Type 316H stainless steel is greatly reduced by the imposition of a 1-min tensile hold, even in the presence of a biaxial stress field. The resulting fracture is predominantly intergranular. The fatigue life of Incoloy 800, on the other hand, is not significantly reduced by the imposition of a 1-min tensile hold, either with or without internal pressure. In contrast to Type 316H stainless steel, Incoloy 800 shows predominantly transgranular fracture in this case.

ACKNOWLEDGMENTS

The author would like to thank M. D. Gorman, W. F. Burke and D. E. Busch for their help in conducting the test program.

REFERENCES

1. S. Majumdar, "Biaxial Creep-fatigue Behavior of Type 316H Stainless Steel Tube," Argonne National Laboratory Report ANL-79-33 (1979).

2. W. Jones, Sandia Laboratories, Albuquerque, New Mexico, personal communication (1979).

3. D. R. Diercks, "A Compilation of United States and British Elevated-Temperature, Strain Controlled Fatigue Data on Type 316 Stainless Steel," Argonne National Laboratory Report ANL/MSD-78-4 (1978).

4. S. Majumdar, "Compilation of Fatigue Data for Incoloy 800 Alloys," Argonne National Laboratory Report ANL/MSD-78-3 (1978).

Distribution for ANL-80-34

Internal:

W. E. Massey
B. R. T. Frost
J. J. Roberts
E. J. Croke
W. W. Schertz
A. A. Jonke
S. Majumdar (20)
D. T. Raske
P. S. Maiya
W. J. Shack
W. F. Burke
D. E. Busch
M. D. Gorman
E. M. Stefanski (4)
A. B. Krisciunas
ANL Contract File
ANL Libraries (5)
TIS Files (6)

External:

DOE-TIC, for distribution per UC-62c (347)
Manager, Chicago Operations and Regional Office, DOE
Chief, Office of Patent Counsel, DOE-CORO
President, Argonne Universities Association
Materials Science Division Review Committee:
- E. A. Aitken, General Electric Co., Sunnyvale
- G. S. Ansell, Rensselaer Polytechnic Inst.
- R. W. Balluffi, Massachusetts Inst. Technology
- R. J. Birgeneau, Massachusetts Inst. Technology
- S. L. Cooper, U. Wisconsin, Madison
- C. Laird, U. Pennsylvania
- M. T. Simnad, General Atomic
- C. T. Tomizuka, U. Arizona
- A. R. C. Westwood, Martin Marietta Labs.

I. Berman, Foster Wheeler Development Corp., Livingston, N. J.
B. Butler, Solar Energy Research Inst.
H. Cobb, Solar Energy Research Inst.
G. D. Gupta, Foster Wheeler Development Corp., Livingston, N. J.
W. B. Jones, Sandia Lab., Albuquerque
C. W. Moore, Sandia Lab., Livermore
T. V. Narayanan, Foster Wheeler Development Corp., Livingston, N. J.
S. Pohlman, Solar Energy Research Inst.
C. N. Spalaris, General Electric Co., San Jose
J. Swearingen, Sandia Lab., Livermore
T. Tracey, Martin Marietta Aerospace, Denver